Article ID: 1000-7032(2014)11-1297-09

Plasmon Excitation in Nitrogen-doped Graphene Nanostructures

YIN Hai-feng[1*], CHEN Guang-ping[1], XIANG Gong-zhou[1], ZHANG Hong[2*]

(1. *College of Physics and Electronic Engineering, Kaili University, Guizhou* 556011, *China*;
2. *College of Physical Science and Technology, Sichuan University, Chengdu* 610065, *China*)

* *Corresponding Authors, E-mail: yinhaifeng*1212@126.*com*; *hongzhang@scu.edu.cn*

Abstract: Plasmon characteristics in nitrogen-doped graphene nanostructures are studied by time-dependent density functional theory. The pyridinic-nitrogen doping does not affect plasmon characteristics of graphene nanostructures, while the substitutional-nitrogen doping affects plasmon resonances of graphene nanostructures due to two main competing factors: The reduced symmetry of graphene nanostructures and the increase of the electron densities. After doped with substitutional-nitrogen, low-energy spectra of hexagonal graphene nanostructures are red-shifted. For rectangular graphene nanostructures, along the armchair-edge direction, the main low-energy spectra always show blue-shifts. However, along the zigzag-edge direction, the substitutional-nitrogen doping has little effect on the main lower-energy collective excitation.

Key words: plasmon; nitrogen-doped graphene nanostructures; time-dependent density functional theory
CLC number: O482.31; O611.4 **Document code**: A **DOI**: 10.3788/fgxb20143511.1297

氮掺杂石墨烯纳米结构的等离激元激发

尹海峰[1*], 陈广萍[1], 向功周[1], 张 红[2*]

(1. 凯里学院 物理与电子工程学院, 贵州 凯里 556011; 2. 四川大学 物理科学与技术学院, 四川 成都 610065)

摘要: 基于含时密度泛函理论,研究了氮掺杂石墨烯纳米结构的等离激元特性。吡啶型氮掺杂不影响石墨烯纳米结构的等离激元激发特性,而取代型氮掺杂主要基于石墨烯纳米结构对称性的改变和体系中电子密度的增加来影响石墨烯纳米结构的等离激元共振。相对于纯六角石墨烯纳米结构,在低能共振区,取代型氮掺杂六角石墨烯纳米结构的等离激元共振能量发生了红移。相对于纯矩形石墨烯纳米结构,在低能共振区,取代型氮掺杂矩形石墨烯纳米结构沿扶手椅型边界方向激发时,其等离激元共振能量发生了蓝移;沿 Z 字型边界激发时,其主要的等离激元共振模式受掺杂氮的影响较小。

关 键 词: 等离激元; 氮掺杂石墨烯纳米结构; 含时密度泛函理论

1 Introduction

Plasmons have been identified in many different systems, ranging from metallic films down to nanoparticles and carbon molecules[1-7]. More recently, plasmons have also been identified in graphene[8-11].

收稿日期: 2014-07-25; **修订日期**: 2014-08-09
基金项目: 国家自然科学基金(11464023,11474207); 贵州省科技厅基金(黔科合 J 字[2012]2299 号,黔科合 J 字 LKK[2013]19 号)资助项目

Compared with plasmons in metals, plasmons in graphene have more advantages[8,10]. Thereinto, the carrier density of graphene can be tuned *via* electrostatic gating or chemical doping, which provides the highly desired feature of tunability to plasmonic materials. These advantages make graphene a very promising plasmonic material that can complement existing plasmonic materials in a broad electromagnetic spectrum range. Though electrostatic gating is one well-established method, chemical doping can potentially achieve the required control without the use of external voltages. Therefore, in chemical doped graphene, tunable plasmons have been received more and more attention[12]. Nitrogen is considered to be an excellent element for the chemical doping of graphene because it has comparable atomic size and contains five valence electrons for bonding with carbon atoms[13-14]. In monolayer graphene, experimentally, different methods have been successfully used to control the nitrogen doping concentration and configuration[15-18]. Theoretically, the stable configuration and the unique electronic properties of nitrogen-doped graphene have also been studied[19]. These studies indicate that nitrogen-doped graphene is the promising optical and electronic devices[19].

Recently, people pay more and more attention to the nitrogen-doped graphene nanostructures (NDGN) due to its marvelous properties associated with quantum-confinement and edge effects[20]. Experimentally, significant advancement has been made in the synthesis of NDGN[21-24]. For example, Li *et al* developed a hydrothermal approach for the synthesis of NDGN by cutting N-doped graphene[17]. They also investigated optical properties of the NDGN and found that, in the NDGN, the photoluminescence blue shift. Jin *et al* successfully fabricated another kind NDGN which are functionalized with amine groups[24]. However, these NDGN exhibit a redshift of photoluminescence emission compared to the pristine graphene quantum dot. Therefore, the influence of the nitrogen doping on optical properties of graphene quantum dots is still not very clear. Moreover, these studies mainly investigated the influence of nitrogen doping concentrations on optical properties of NDGN. The shape of NDGN and the nitrogen doping configuration have not been taken into account, whereas they will have an important impact on the optical characteristics of the nanostructures.

In this paper, we investigated collective excitations in NDGN using time-dependent density functional theory. Geometries of NDGN which we discussed are rectangular and hexagonal. The dangling σ bonds at the edges are passivated by hydrogen atoms. We mainly studied the impacts of the nitrogen doping configuration and the shapes of NDGN on the plasmon resonance characteristics. We also discussed the effect of nitrogen doping concentrations and the reduced symmetry. Firstly, we studied the plasmon excitation in the pyridine-like nitrogen-doped graphene nanostructure. Then, we investigated the plasmon excitation in the substitutional nitrogen-doped graphene nanostructure.

2 Computational Methods

All of our calculations were performed with time-dependent density functional theory code OCTOPUS[25-26]. Time-dependent density functional theory has successfully predicted the collective excitation of the electron in carbon-based nanomaterials[27-30]. In our calculations, carbon atom and hydrogen atom were described by the Troullier-Martins pseudopotentials[31]. Local density approximation (LDA)[32] for the exchange-correlation was used in both the ground state and excited state calculations as employed by Marinopoulos *et al*[28]. The simulation zone was defined by assigning a sphere around each atom with a radius of 0.9 nm and a uniform mesh grid of 0.03 nm. In the real time propagation, excitation spectrum was extracted by Fourier transform of the dipole strength induced by an impulse excitation[33]. At the same time, we also could obtain the response to the particular polarization. This scheme has been used before in predicting collective excitations of small sodium clusters with linear structures[34]. In the real-time propagation, the electronic wave packets were evolved for typically 8 000

steps with a time step of $\Delta t = 0.005$ ħ/eV. We use Cartesian coordinates and fix atoms in XY plane. For the rectangular graphene nanostructures, the zigzag-edge is perpendicular to X-axis, while the armchair-edge is parallel to X-axis, as shown in Fig. 1. For the hexagonal graphene nanostructures with zigzag-edges, two edges are perpendicular to X-axis. We mainly investigate the plasmon excitation in the direction that is parallel to the plane of the graphene nanostructure.

3 Results and Discussion

Fig. 1 shows dipole responses (Optical absorptions) of the pyridine-like nitrogen-doped graphene nanostructures to an impulse excitation polarized in X-axis and Y-axis directions respectively. The insets are schematic diagrams of the pyridine-like nitrogen-doped hexagonal and rectangular graphene nanostructures. The light gray ball denotes the hydrogen atom; the gray ball denotes the carbon atom; the ring denotes the nitrogen atom. Compared with the dipole response of the pristine graphene nanostructure[35], the results of Fig. 1 (a) show that line profiles of absorption spectra of the pyridine-like nitrogen-doped graphene A nanostructure and the pristine graphene nanostructure are the same, and absorption peak positions are also almost identical. This phenomenon is similar to the relationship between the absorption spectra of pyridine and benzene. The study of Bene *et al* shows that the pyridine spectrum closely resembles that of benzene[36]. The presence of the nitrogen atom in pyridine can be viewed as a perturbation on the benzene system. In our study, we also investigated the absorption spectra of pyridine and benzene by TDDFT, and our result is in line with previous theoretical and experimental studies[36-38]. Therefore, these indicate that, for the nitrogen-doped graphene nanostructures, calculation results of TDDFT should be reasonable.

Then, we studied the evolution of collective excitations in the pyridine-like hexagonal graphene nanostructures with the increase of the number of nitrogen atoms, and found that the absorption spectra of these nanostructures are almost identical as shown in Fig. 1 (a) and (b). In the pyridine-like hexagonal graphene nanostructures, different number of nitrogen atoms has little effect on plasmon excitation characteristics. Meanwhile, we also found that, in

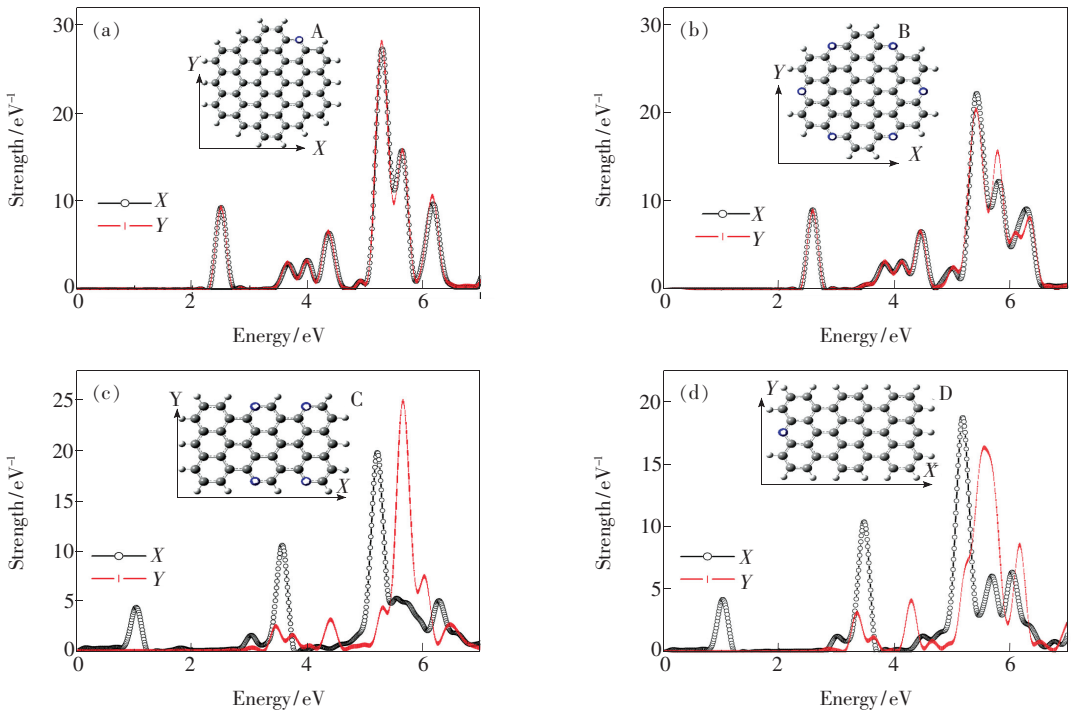

Fig. 1　Dipole responses (Optical absorptions) of the pyridine-like nitrogen-doped graphene nanostructures to an impulse excitation polarized in X-axis and Y-axis directions. The insets are schematic diagrams of these nanostructures, respectively.

X-axis and *Y*-axis directions, absorption spectra of the pyridine-like nitrogen-doped hexagonal graphene nanostructures are still almost identical. Symmetric and asymmetric doping has no impact on the absorption spectra as shown in Fig. 1 (a) and (b). It should be noted that, with the increase of the number of nitrogen atoms, in the lower-energy resonance zone, absorption spectra are blue-shifted a little. This is due to the relative increase of the π electron density. For example, the low-energy absorption peak of the pyridine-like nitrogen-doped graphene A nanostructure is located in 2.5 eV, while the low-energy absorption peak of the pyridine-like nitrogen-doped graphene B nanostructure is located in 2.58 eV. Moreover, we investigated optical absorptions of the pyridine-like rectangular graphene nanostructures as shown in Fig. 1(c) and (d). Comparing with our previous study on the pristine rectangular graphene nanostructure[35], we found that, to an impulse excitation polarized in *X*-axis or *Y*-axis directions, line profiles of absorption spectra of the pyridine-like rectangular graphene nanostructures and the pristine rectangular graphene nanostructure are the same, and the absorption peak positions are also almost identical. The pyridinic-nitrogen doping at any boundary, has almost no impact on the absorption spectra of rectangular graphene nanostructures. These results show that the pyridinic nitrogen dopant does not affect the plasmon excitation characteristic of the graphene nanostructures.

In order to further elucidate whether the pyridinic nitrogen dopant has an impact on the plasmon excitation characteristic of the graphene nanostructures, we studied the Fourier transform of the induced charge density for the pyridine-like nitrogen-doped graphene B nanostructure which is shown in Fig. 1 (b). Fig. 2 shows the Fourier transform of the induced density, obtained from time-evolution, in a plane, at the energy resonance points 2.58 eV (a) and 4.46 eV (b) respectively. The polarization direction is along *X*-axis direction. The induced density plane is parallel to the graphene nanostructure plane, and the vertical distance between the graphene nanostructure plane and this induced density plane is 0.09 nm. We mainly calculated the induced charge response of the lower-energy resonance zone. In our previous studies[35], we also investigated the Fourier transform of the induced charge density for the pristine graphene nanostructure, at the energy resonance points 2.48 eV and 4.35 eV, respectively. By comparing, we found that, for the pristine graphene nanostructure and the pyridine-like nitrogen-doped graphene B nanostructure, the Fourier transform of the induced charge density are almost identical at the corresponding energy resonance points. For the pyridine-like nitrogen-doped graphene B nanostructure, the induced charges of the lower-energy resonance points are still distributed in the boundary region, and the induced density profile for these plasmon resonance points still has the dipole-like feature. This is because the lower-energy plasmon is a long-range charge transfer excitation. Along the excitation direction, the electrons can move back and forth. The results of Fig. 2 again indicate that the pyridinic nitrogen dopant has no impact on the plasmon excitation characteristic of the graphene nanostructures.

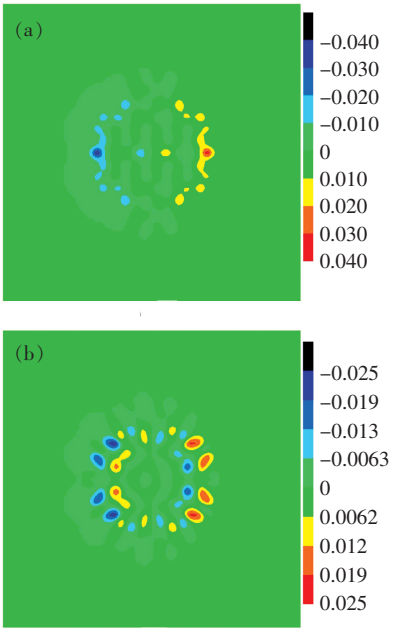

Fig. 2 Fourier transform of the induced charge density for pyridine-like nitrogen-doped graphene B nanostructure of Fig. 1(b). The polarization direction is along *X*-axis direction, at the energy resonance points 2.58 eV (a) and 4.46 eV (b), respectively.

Fig. 3 shows optical absorptions of the substitutional nitrogen-doped hexagonal graphene nanostructures (SNHGN) to an impulse excitation polarized in *X*-axis and *Y*-axis directions, respectively. The insets are schematic diagrams of SNHGN. According to the previous study of density functional theory (DFT)[19], these SNHGN which we studied are relatively stable nanostructures. The results of Fig. 3 demonstrate that absorption spectra of SNHGN have some common characteristics. Compared with the pristine hexagonal graphene nanostructure[35], along *X*-axis and *Y*-axis directions, all low-energy absorption spectra are red-shifted. In the classical free-electron or Drude model[34], absorption spectra will be blue-shifted with the increase of the electron density. However, for SNHGN, compared with the pristine hexagonal graphene nanostructure, the electron density of the nanostructures relatively increases, while absorption spectra of the nanostructures are red-shifted. On the one hand, we argue this phenomenon is mainly because, after doped with nitrogen, the relatively higher-symmetry of the nanostructures goes down. On the other hand, we argue the red-shift of absorption spectra is also resulted from the impact of the potential surface changes brought by doping nitrogen.

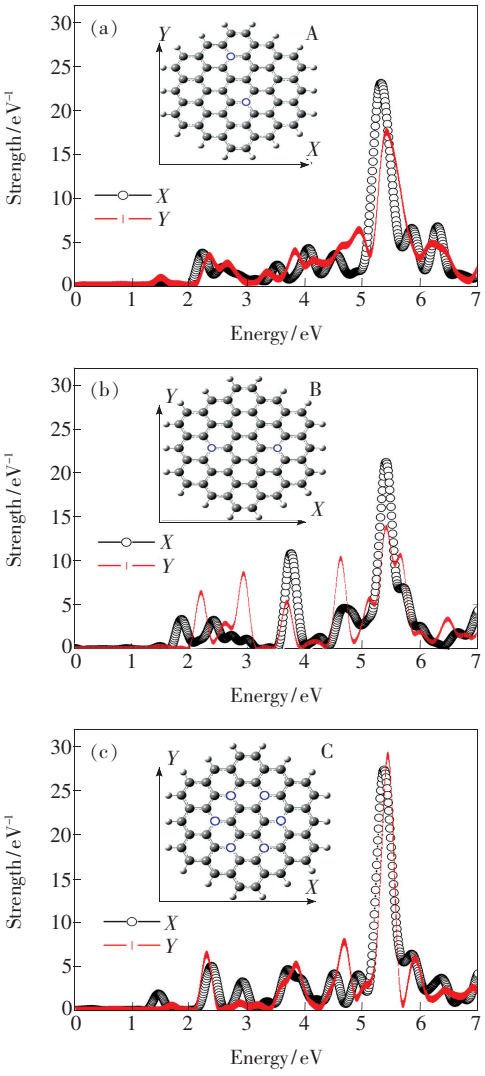

Fig. 3　Optical absorptions of the substitutional nitrogen-doped hexagonal graphene nanostructures to an impulse excitation polarized in *X*-axis and *Y*-axis directions. The insets are schematic diagrams of the substitutional nitrogen-doped hexagonal graphene nanostructures, respectively.

To elucidate the impact of substitutional nitrogen doping on the plasmon excitation characteristic of the graphene nanostructures, we studied the Fourier transform of the induced charge density for the substitutional nitrogen-doped hexagonal graphene C nanostructure which is shown in Fig. 3. Fig. 4(a) and (b) show the Fourier transform of the induced charge density, obtained from time-evolution, in a plane at the energy resonance points 1.87 eV (a) and 2.21 eV (b), respectively. The polarization direction of Fig. 4(a) is in *X*-axis direction, while the polarization direction of Fig. 4(b) is in *Y*-axis direction. The results show that, when the nitrogen atom is doped in the center region, the low-energy plasmon resonance modes of graphene nanostructures are greatly affected. Compared with the pristine graphene nanostructure[35], the induced charges of these lower-energy resonance points are not only distributed in the boundary region, but also distributed in the center region. The result indicates that the change of potential field of the center region has an important impact on the low-energy plasmon resonance modes. Moreover, in the center region, the induced charge density of Fig. 4(b) is larger than the induced charge density of Fig. 4(a). The result shows that, along *Y*-axis and *X*-axis directions, electric potential field changes are different. Because of this characteristic, the extent of the redshift of the spectrum is much greater in *X*-axis direction. This result also demonstrates that, after doped with nitrogen,

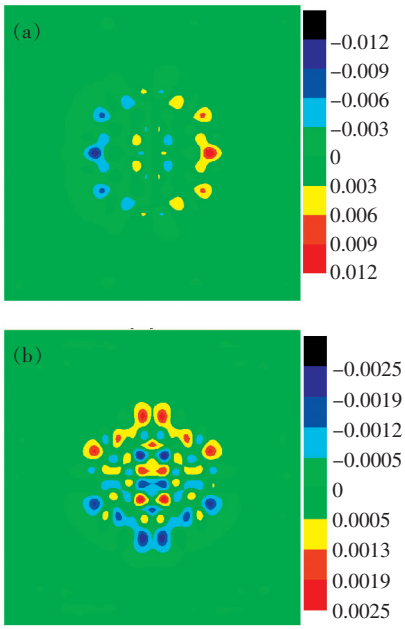

Fig. 4 Fourier transform of the induced charge density for substitutional nitrogen-doped hexagonal graphene C nanostructure of Fig. 3. (a) The polarization direction is along *X*-axis direction, at the energy resonance points 1.87 eV. (b) The polarization direction is along *Y*-axis direction, at the energy resonance points 2.21 eV.

the relatively higher-symmetry of the nanostructures goes down from the perspective of the electric potential field distribution.

Fig. 5 shows optical absorptions of the substitutional nitrogen-doped rectangular graphene nanostructures (SNRGN) to an impulse excitation polarized in *X*-axis and *Y*-axis directions respectively. The insets (A, B, C, and D) are schematic diagrams of SNRGN. Unlike SNHGN, compared with the pristine graphene nanostructure[35], the main absorption peaks of SNRGN are not red-shifted. On the contrary, along the armchair-edge direction, the main lower-energy absorption peaks of SNRGN are blue-shifted. For the original lower symmetry rectangular nanostructures, in the lower-energy resonance zone, the further decrease of the symmetry do not reduce the main plasmon resonance energies. When some of the carbon atoms are replaced with nitrogen atoms, the electron densities of the rectangular nanostructures relatively increase. For this reason, in *X*-axis direction, the main lower-energy absorption peaks of SNRGN are blue-shifted. In order to further elucidate whether the blue shift of spectral

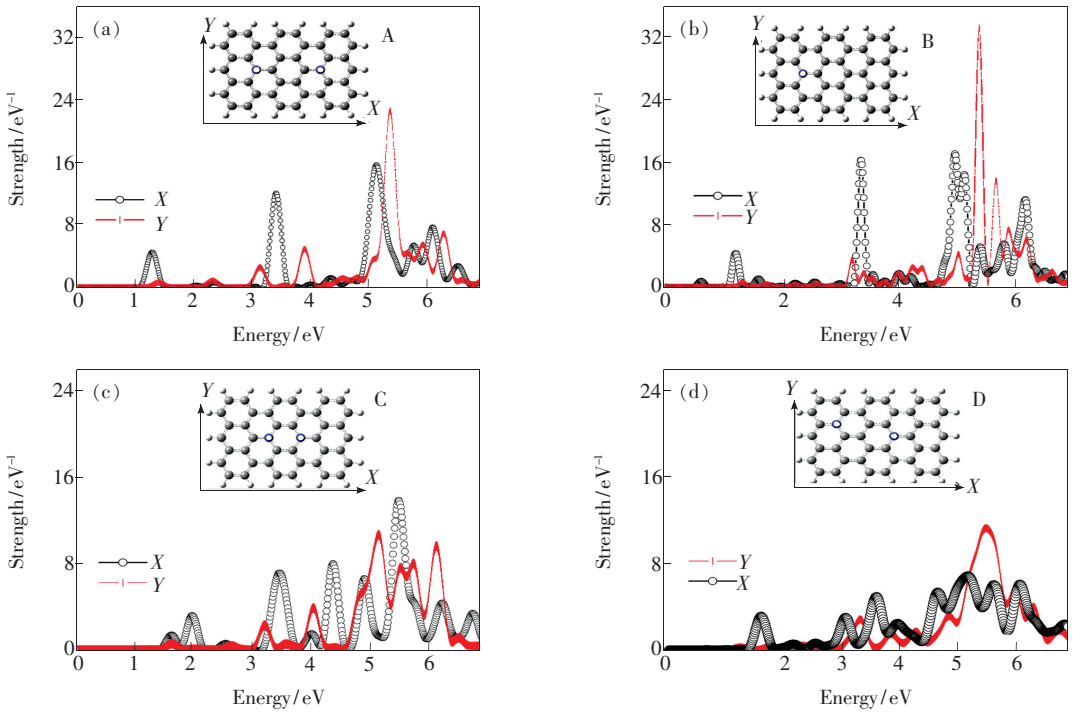

Fig. 5 Optical absorptions of the substitutional nitrogen-doped rectangular graphene nanostructures to an impulse excitation polarized in *X*-axis and *Y*-axis directions. The insets are schematic diagrams of the substitutional nitrogen-doped rectangular graphene nanostructures, respectively.

is due to the relative increase of electron density, we calculated the induced charge response of these lower-energy resonance zone. Fig. 6(a) shows the Fourier transform of the induced charge density for graphene nanostructure A of Fig. 5, obtained from time-evolution, in a plane at the energy resonance points 1.3 eV. The induced density plane is parallel to the graphene nanostructure plane, and the vertical distance between the graphene nanostructure plane and this induced density plane is 0.09 nm. The polarization direction is in *X*-axis direction. Compared with the pristine graphene nanostructure[35], the low-energy plasmon resonance mode of graphene nanostructures is not changed. The induced charge is still mainly distributed in the boundary region. However, the difference is that the induced charge density of this nitrogen-doped graphene nanostructure is much larger. This result indicates that, along the armchair-edge direction, the blue shift of the lower-energy absorption peaks of SNRGN is mainly due to the relative increase of electron density. For the impulse excitation polarized in the zigzag-edge direction, compared with the pristine graphene nanostructure[35], there are very small absorption peaks in the lower-energy resonance zone. More interestingly, for different positions of nitrogen-doped, the main lower-energy absorption peak of SNRGN almost does not move, and still locates in the vicinity of 3.14 eV. Fig. 6 (b) shows the Fourier transform of the induced charge density for graphene nanostructure A of Fig. 5, in a plane at the energy resonance points 3.14 eV. The polarization direction is in zigzag-edge direction. Compared with the pristine rectangular graphene nanostructure[35], the distribution of the induced charge density of the main lower-energy plasmon resonance mode of SNRGN has a little change because the electronegativity of nitrogen is larger than the electronegativity of carbon, but two induced density profiles are almost identical. Therefore, after doped with nitrogen, in the vicinity of 3.14 eV, the main lower-energy plasmon resonance mode of SNRGN is almost not changed.

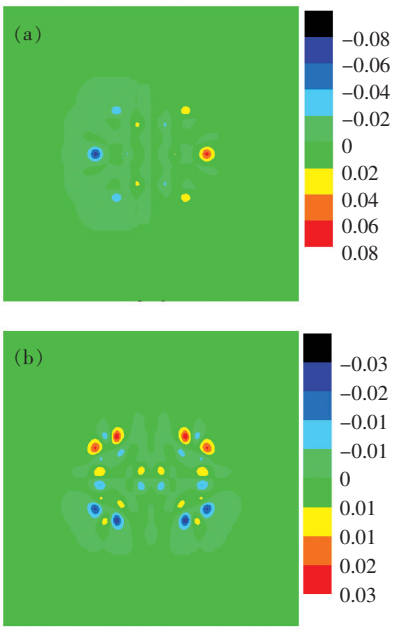

Fig. 6　Fourier transform of the induced charge density for substitutional nitrogen-doped rectangular graphene A nanostructure of Fig. 5. (a) The polarization direction is along *X*-axis direction, at the energy resonance points 1.3 eV. (b) The polarization direction is along *Y*-axis direction, at the energy resonance points 3.14 eV.

4　Conclusion

In conclusion, using time-dependent density functional theory, we have carried out a systematic study of collective excitations of nitrogen-doped graphene nanostructures, and mainly investigated the impacts of the pyridinic and substitutional nitrogen doping on the plasmon excitations. Based on these calculations and results, the following conclusions can be drawn. First of all, the pyridinic nitrogen doping does not affect the plasmon excitation characteristic of graphene nanostructures. Absorption spectra of the pyridine-like nitrogen-doped graphene nanostructure and the pristine graphene nanostructure are almost identical. Second, for substitutional nitrogen doping, the low-energy plasmon resonances of graphene nanostructures mainly depend on the competition between the reduced symmetry of the nanostructures which is brought by doping nitrogen and the relative increase of the electron densities. Compared with the absorption spectrum of the pristine hexagonal graphene nanostructure, low-energy absorption spectra of SNHGN are red-shifted, which is mainly due to the reduced symmetry of the nanostructures.

Unlike SNHGN, along the armchair-edge direction, the main lower-energy absorption peaks of SNRGN are always blue-shifted. The relative increase of the electron densities always plays more important role in plasmon excitations than the decrease of the symmetry of the nanostructures. Moreover, along the zigzag-edge direction, though there are some small absorption peaks in the low energy resonance region, the main lower-energy absorption peak of SNRGN almost does not move. The results show that, in different directions, substitutional nitrogen doping has different effects on the plasmon resonance. Our study paves the way for applications of graphene in sensing, infrared photo-detection, and light modulation.

Acknowledgments: We thank S. W. Gao for his kind help in writing codes.

References:

[1] Ritchie R H. Plasma losses by fast electrons in thin films [J]. *Phys. Rev.*, 1957, 106(5):874-1-4.

[2] Myroshnychenko V, Rodríguez-Fernández J, Pastoriza-Santos I, *et al.* Modelling the optical response of gold nanoparticles [J]. *Chem. Soc. Rev.*, 2008, 37(14):1792-1805.

[3] Kociak M, Henrard L, Stéphan O, *et al.* Plasmons in layered nanospheres and nanotubes investigated by spatially resolved electron energy-loss spectroscopy [J]. *Phys. Rev.* B, 2000, 61(20):13936-13944.

[4] Yang Z L, Fang W, Yang Y Q. Two-photon-excited fluorescence enhancement caused by surface plasmon enhanced exciting light [J]. *Chin. J. Lumin.* (发光学报), 2013, 34(2):240-244 (in Chinese).

[5] Han J, Fan Y C, Zhang Z R. Propagation of surface plasmon polaritons in a ring resonator with PT-symmetry [J]. *Chin. J. Lumin.* (发光学报), 2012, 33(8):901-904 (in Chinese).

[6] Tong L M, Xu H X. Frontiers of plasmonics [J]. *Front. Phys.*, 2014, 9(1):1-2.

[7] Chen Y Y, Tong G Z, Qin L, *et al.* Progress in surface plasmon polariton nano-laser technologies and applications [J]. *Chin. Opt.* (中国光学), 2012, 5(5):453-463 (in Chinese).

[8] Ju L, Geng B, Horng J, *et al.* Graphene plasmonics for tunable terahertz metamaterials [J]. *Nat. Nanotechnol.*, 2011, 6:630-634.

[9] Grigorenko A N, Polini M, Novoselov K S. Graphene plasmonics [J]. *Nat. Photon.*, 2012, 6:749-758.

[10] De Abajo F J G. Graphene nanophotonics [J]. *Science*, 2013, 339(6122):917-918.

[11] Christensen J, Manjavacas A, Thongrattanasiri S, *et al.* Graphene plasmon waveguiding and hybridization in individual and paired nanoribbons [J]. *ACS Nano*, 2012, 6(1):431-440.

[12] Schiros T, Nordlund D, Pálová L, *et al.* Connecting dopant bond type with electronic structure in N-doped graphene [J]. *Nano Lett.*, 2012, 12(8):4025-4031.

[13] Wang Y, Shao Y, Matson D W, *et al.* Nitrogen-doped graphene and its application in electrochemical biosensing [J]. *ACS Nano*, 2010, 4(4):1790-1798.

[14] Lee S U, Belosludov R V, Mizuseki H, *et al.* Designing nanogadgetry for nanoelectronic devices with nitrogen-doped capped carbon nanotubes [J]. *Small*, 2009, 5(15):1769-1775.

[15] Zhao L, He R, Rim K T, *et al.* Visualizing individual nitrogen dopants in monolayer graphene [J]. *Science*, 2011, 333(6045):999-1003.

[16] Gao H, Song L, Guo W, *et al.* A simple method to synthesize continuous large area nitrogen-doped graphene [J]. *Carbon*, 2012, 50(12):4476-4482.

[17] Li M, Wu W, Ren W, *et al.* Synthesis and upconversion luminescence of N-doped graphene quantum dots [J]. *Appl. Phys. Lett.*, 2012, 101(10):103107-1-3.

[18] Guo B, Liu Q, Chen E, *et al.* Controllable N-doping of graphene [J]. *Nano Lett.*, 2010, 10(12):4975-4980.

[19] Xiang H J, Huang B, Li Z Y, *et al.* Ordered semiconducting nitrogen-graphene alloys [J]. *Phys. Rev.* X, 2012, 2(1):011003-1-7.

[20] Ritter K A, Lyding J W. The influence of edge structure on the electronic properties of graphene quantum dots and nanoribbons [J]. *Nat. Mater.*, 2009, 8:235-242.

[21] Yan X, Cui X, Li B, *et al.* Large, solution-processable graphene quantum dots as light absorbers for photovoltaics [J].

Nano Lett., 2010, 10(5):1869-1873.

[22] Yan X, Cui X, Li L. Synthesis of large, stable colloidal graphene quantum dots with tunable size [J]. *J. Am. Chem. Soc.*, 2010, 132(17):5944-5945.

[23] Li Y, Zhao Y, Cheng H, *et al.* Nitrogen-doped graphene quantum dots with oxygen-rich functional groups [J]. *J. Am. Chem. Soc.*, 2012, 134(1):15-18.

[24] Jin S H, Kim D H, Jun G H, *et al.* Tuning the photoluminescence of graphene quantum dots through the charge transfer effect of functional groups [J]. *ACS Nano*, 2013, 7(2):1239-1245.

[25] Marques M A L, Castro A, Bertsch G F, *et al.* Octopus: A first-principles tool for excited electron-ion dynamics [J]. *Comput. Phys. Commun.*, 2003, 151(1):60-78.

[26] Castro A, Appel H, Oliveira M, *et al.* Octopus: A tool for the application of time-dependent density functional theory [J]. *Phys. Stat. Sol.* (b), 2006, 243(11):2465-2469.

[27] Rubio A, Alonso J A, Lopez J M, *et al.* Surface plasmon excitations in C_{60}, $C_{60}K$ and $C_{60}H$ clusters [J]. *Phys.* B, 1993, 183(3):247-263.

[28] Marinopoulos A G, Reining L, Olevano V, *et al.* Anisotropy and interplane interactions in the dielectric response of graphite [J]. *Phys. Rev. Lett.*, 2002, 89(7):076402-1-4.

[29] Marinopoulos A G, Reining L, Rubio A, *et al.* Optical and loss spectra of carbon nanotubes: Depolarization effects and intertube interactions [J]. *Phys. Rev. Lett.*, 2003, 91(4):046402-1-4.

[30] Despoja V, Novko D, Dekanić K, *et al.* Two-dimensional and π plasmon spectra in pristine and doped graphene [J]. *Phys. Rev.* B, 2013, 87(7):075447-1-10.

[31] Troullier N, Martins J L. Efficient pseudopotentials for plane-wave calculations [J]. *Phys. Rev.* B, 1992, 43(3):1993-2006.

[32] Ceperley D M, Alder B J. Ground state of the electron gas by a stochastic method [J]. *Phys. Rev. Lett.*, 1980, 45(7):566-569.

[33] Yabana K, Bertsch G F. Time-dependent local-density approximation in real time [J]. *Phys. Rev.* B, 1996, 54(7):4484-4487.

[34] Yan J, Yuan Z, Gao S. End and central plasmon resonances in linear atomic chains [J]. *Phys. Rev. Lett.*, 2007, 98(21):216602-1-4.

[35] Yin H F, Zhang H. Plasmons in graphene nanostructures [J]. *J. Appl. Phys.*, 2012, 111(10):103502-1-6.

[36] Bene J D, Jaffé H H. Use of the CNDO method in spectroscopy. I. benzene, pyridine, and the diazines [J]. *J. Chem. Phys.*, 1986, 48(6):1807-1812.

[37] Yabana K, Bertsch G F. Time-dependent local-density approximation in real time: Application to conjugated molecules [J]. *Int. J. Quantum Chem.*, 1999, 75(1):55-66.

[38] Koch E E, Otto A. Optical absorption of benzene vapour for photon energies from 6 eV to 35 eV [J]. *Chem. Phys. Lett.*, 1972, 12(3):476-480.

尹海峰(1982 -),男,河南汝南人,博士,副教授,2013 年于四川大学获得博士学位,主要从事团簇及纳米材料中的等离激元方面的研究。
E-mail: yinhaifeng1212@126.com

张红(1967 -),女,四川成都人,博士,教授,2004 年于四川大学获得博士学位,主要从事凝聚态物理的基础理论和计算方面的研究。
E-mail: hongzhang@scu.edu.cn